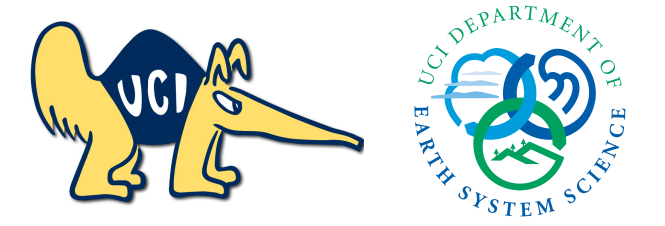


Nonlinear Interactions between Climate and Atmospheric Carbon Dioxide Drivers of Terrestrial and Marine Carbon Cycle Changes from 1850 to 2300

Forrest M. Hoffman^{1,2}, James T. Randerson¹, J. Keith Moore¹, Michael Goulden¹, Keith Lindsay⁶, Ernesto Muñoz⁶, Weiwei Fu¹, Abigail L. S. Swann³, Charles D. Koven⁴, Natalie Mahowald⁵, and Gordon B. Bonan⁶

ICDC10 Poster
Session 5, #375
CLIMATE CHANGE
SCIENCE INSTITUTE
OAK RIDGE NATIONAL LABORATORY

¹Department of Earth System Sciences, University of California, Irvine, California 92697, USA; ²Computational Earth Sciences Group, Oak Ridge National Laboratory, Oak Ridge, Tennessee 37831, USA; ³Department of Atmospheric Sciences and Department of Biology, University of Washington, Seattle, WA 98195-1640, USA; ⁴Earth Sciences Division, Lawrence Berkeley National Laboratory, Berkeley, CA 94720, USA; ⁵Earth and Atmospheric Sciences, Cornell University, Ithaca, New York 14853, USA; and ⁶Climate & Global Dynamics Division, National Center for Atmospheric Research, Boulder, Colorado 80307, USA



Introduction

- Quantifying carbon cycle feedbacks with Earth's climate system is important for predicting future atmospheric CO₂ levels and informing carbon management and energy policies.
- We applied a feedback analysis framework to three sets of long-term climate change simulations to quantify drivers of terrestrial and ocean responses of carbon uptake.
- We found that the strength of the climate-carbon cycle feedback gain (g) was dependent upon the type of simulation used to derive the temperature sensitivity parameters (γ).

Methods

Simulations were performed with the NSF-DOE Community Earth System Model version 1.0 (CESM1(BGC)) for three different radiative and biosphere coupling configurations without land use change. The standard protocol from the Fifth Phase of the Coupled Modeling Intercomparison Project (CMIP5) was followed for the period 1850–2300:

- Historical for 1850–2005,
- Representative Concentration Pathway 8.5 (RCP8.5) for 2006–2100, and
- Extended Concentration Pathway 8.5 (ECP8.5) for 2101–2300.

All three simulations were forced with the same prescribed CO₂ mole fraction trajectory as shown in Figure 1(a).

Table 1: Three 451-y CESM1(BGC) simulations, employing different coupling configurations, were analyzed.

Simulation Identifier	Radiative Coupling		Biosphere Coupling	
	CO ₂	Other GHG & aerosols	CO ₂ deposition	Land use change
RAD	✓	✓	✓	✓
BGC	✓	✓	✓	✓
FC	✓	✓	✓	✓

Schwinger *et al.* (2014) derived formulas for calculating feedback parameters from a pair of model experiments. The concentration-carbon feedback parameters can be determined from the FC and RAD simulations as follows,

$$\beta_{FC-RAD} = \frac{\Delta C_{FC}^{\Delta T_{RAD}} - \Delta C_{RAD}^{\Delta T_{FC}}}{\Delta C_{FC}^{\Delta T_{RAD}} - \Delta C_{RAD}^{\Delta T_{FC}}}, \quad (1)$$

and the FC and BGC simulations can be used to derive the climate-carbon feedback parameters as follows,

$$\gamma_{FC-BGC} = \frac{\Delta C_{BGC}^{\Delta T_{FC}} - \Delta C_{FC}^{\Delta T_{BGC}}}{\Delta T_{BGC}^{\Delta T_{FC}} - \Delta T_{FC}^{\Delta T_{BGC}}}. \quad (2)$$

The overall climate-carbon feedback gain (g) can be related to feedback sensitivity parameters as follows,

$$g = \frac{-\alpha(\gamma_O + \gamma_L)}{(m + \beta_O + \beta_L)}, \quad (3)$$

where α is the sensitivity of the global mean near-surface air temperature to cumulative changes in atmospheric CO₂ in units of K ppm⁻¹, m is a constant (2.12 Pg C ppm⁻¹).

We developed a metric to gauge the nonlinearity of drivers and model responses as follows,

$$M_{NL} = 1 - \frac{(\Delta RAD + \Delta BGC)}{\Delta FC}. \quad (4)$$

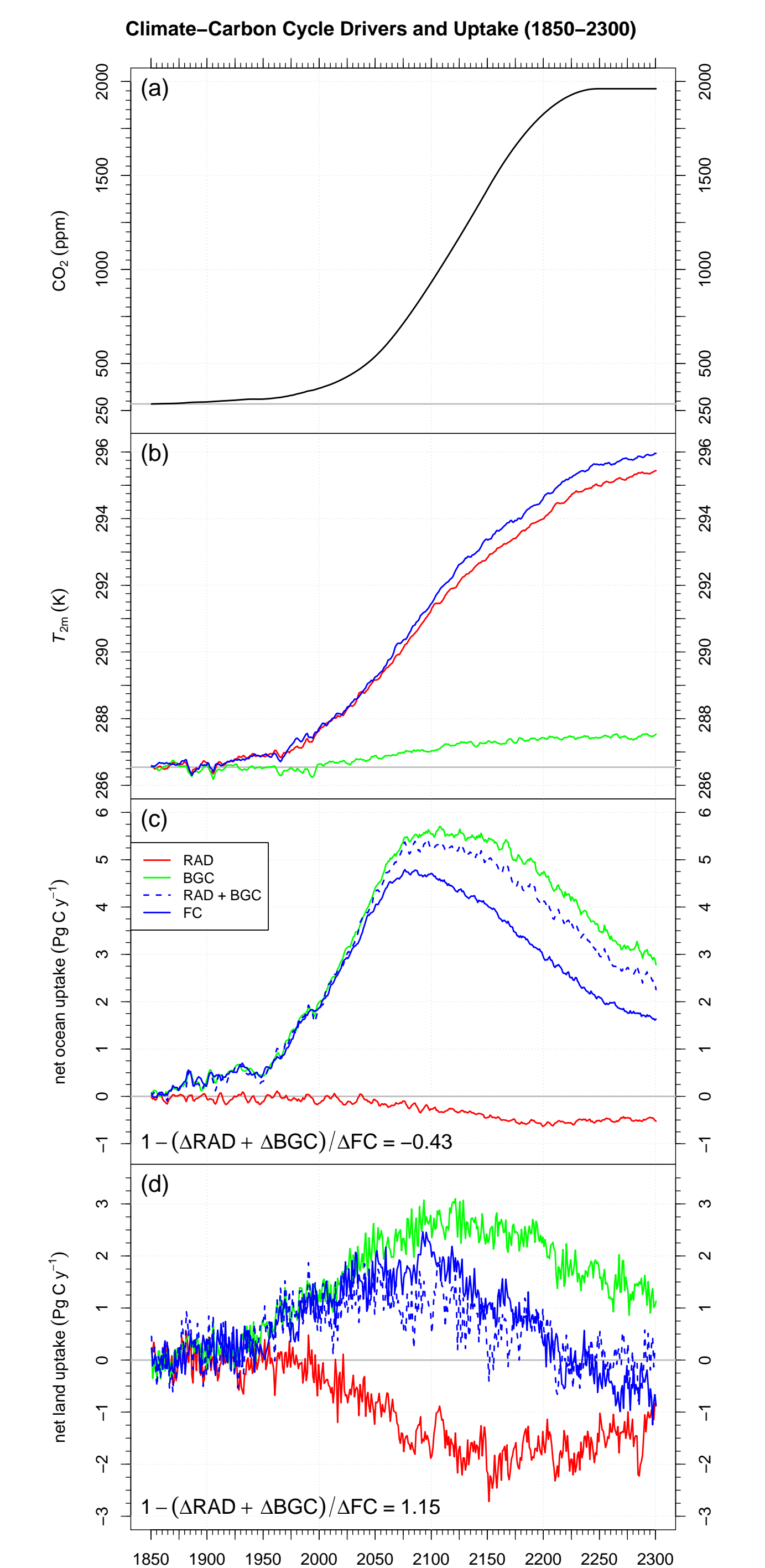


Figure 1: (a) The prescribed atmospheric CO₂ mole fraction was stabilized at 1962 ppm after 2225. (b) Near-surface air temperature increased in all three simulations by the end of the 23rd century. (c) Net ocean uptake decreased in the RAD simulation, but increased in the BGC and FC simulations. (d) Net land uptake was more variable than net ocean uptake, and it increased in the BGC and FC simulations and decreased in the RAD simulation.

Climate-Carbon Cycle Feedback Analysis

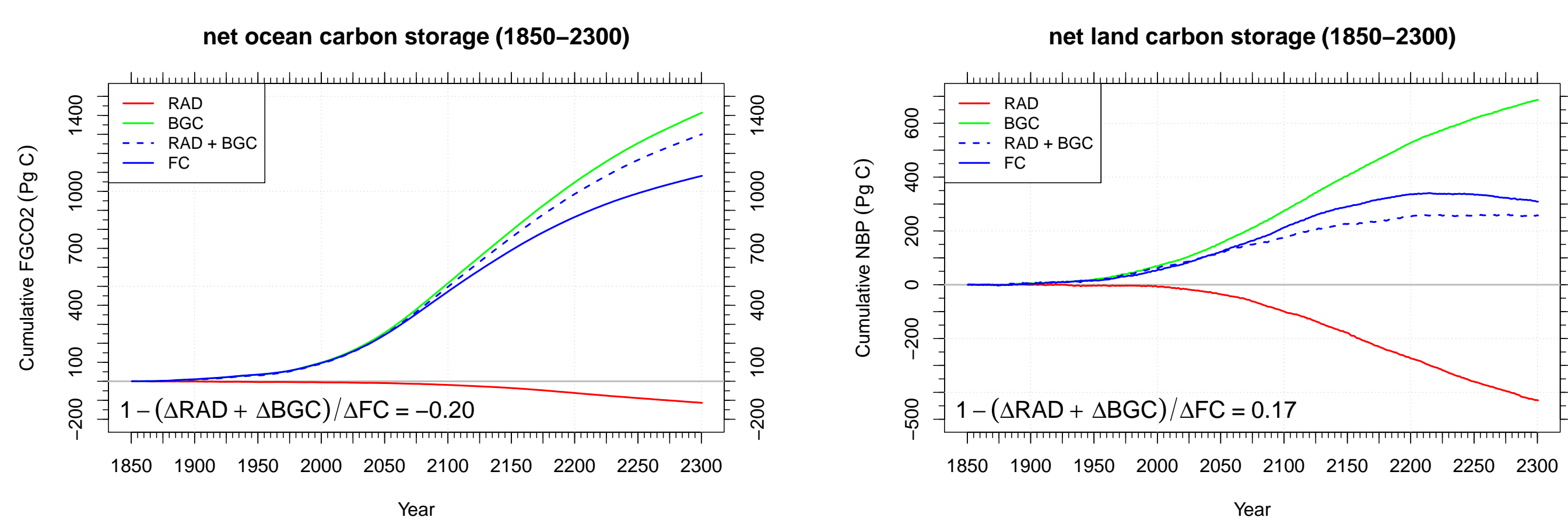


Figure 2: (a) Net ocean carbon storage, integrated from 1850 to 2300, for the BGC simulation was 1414 Pg C, for the FC simulation was 1082 Pg C, and for the RAD simulation was -113 Pg C. (b) Net land carbon storage, integrated from 1850 to 2300, for the BGC simulation was 687 Pg C, for the FC simulation was 309 Pg C, and for the RAD simulation was -430 Pg C.

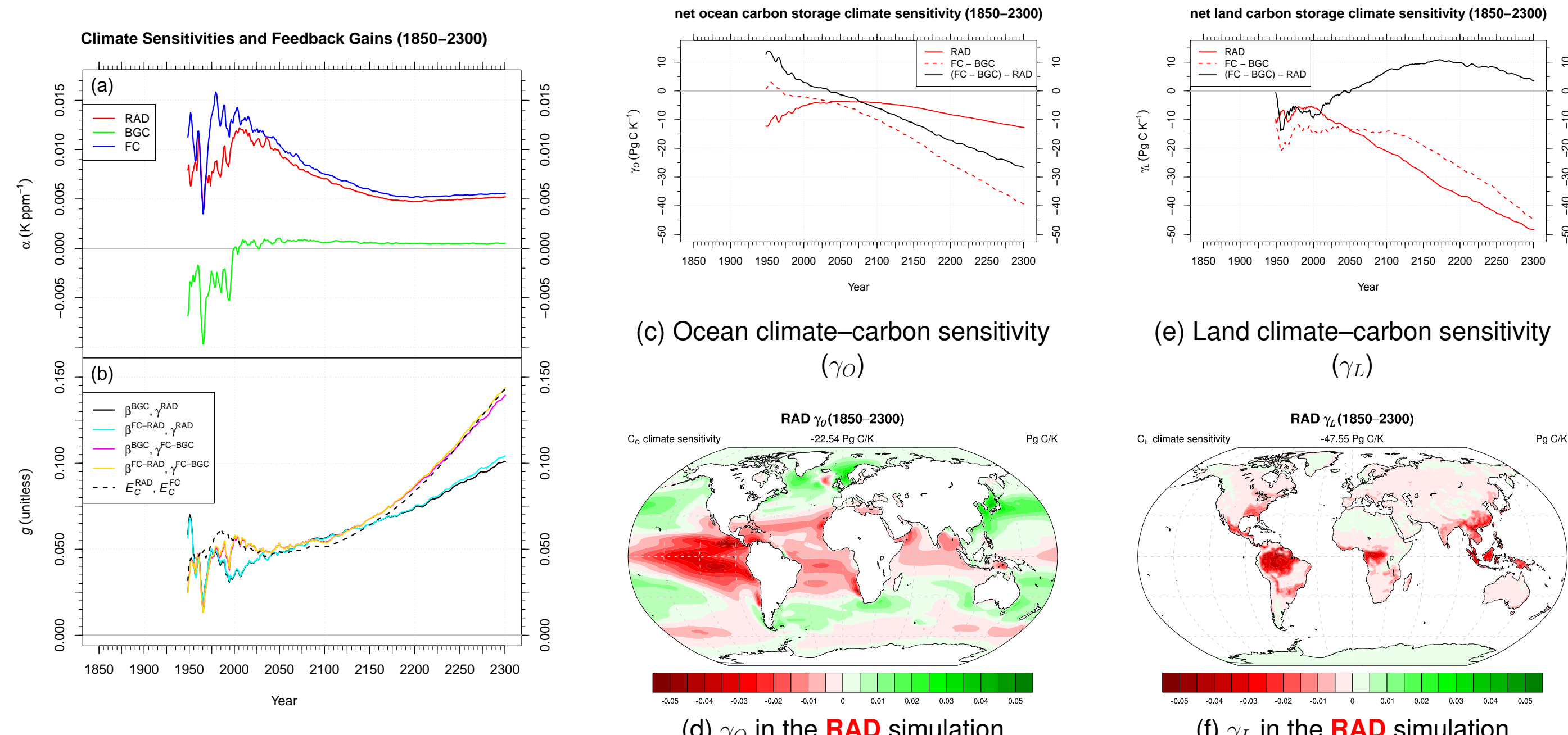


Figure 3: (a) The climate sensitivity (α) for the FC simulation was about 0.0056 K ppm⁻¹ at the end of the 23rd century. (b) The climate-carbon cycle feedback gain (g) clustered around two different values, depending on the method and experiments used to calculate it. (c), (d) The climate-carbon sensitivity, γ_O^{RAD} , was -12.69 Pg C K⁻¹ at the end of the 23rd century. (e), (f) The land climate-carbon sensitivity, γ_L , was -48.25 Pg C K⁻¹ at the end of the 23rd century.

Table 2: Temperature & C changes and compatible emissions.

Variable	Time (year)		
	2100	2200	2300
[CO ₂] _A (ppm)	936	1829	1962
Variable	Time Period (years)		
	1850–2100	1850–2200	1850–2300
$\Delta T_{2m}^{\text{RAD}}$ (K)	4.76	7.46	8.90
$\Delta T_{2m}^{\text{BGC}}$ (K)	0.50	0.87	0.99
$\Delta T_{2m}^{\text{FC}}$ (K)	4.92	8.11	9.41
ΔC_O^{RAD} (Pg C)	-19	-62	-113
ΔC_O^{BGC} (Pg C)	519	1050	1414
ΔC_O^{FC} (Pg C)	475	866	1082
ΔC_L^{RAD} (Pg C)	-100	-275	-430
ΔC_L^{BGC} (Pg C)	276	529	687
ΔC_L^{FC} (Pg C)	213	336	309
E_C^{BGC} (Pg C)	2180	4862	5663
E_C^{FC} (Pg C)	2072	4486	4955

Table 3: Climate-carbon cycle feedback parameters and gains.

Parameter	Time Period (years)		
	1850–2100	1850–2200	1850–2300
α (K ppm ⁻¹)	0.0075	0.0052	0.0056
β_{O}^{BGC} (Pg C ppm ⁻¹)	0.80	0.68	0.84
$\beta_{O}^{\text{FC-RAD}}$ (Pg C ppm ⁻¹)	0.76	0.60	0.71
β_{O}^{FC} (Pg C ppm ⁻¹)	0.42	0.34	0.41
$\beta_{L}^{\text{FC-RAD}}$ (Pg C ppm ⁻¹)	0.48	0.39	0.44
γ_O^{RAD} (Pg C K ⁻¹)	-4.06	-8.26	-12.69
$\gamma_O^{\text{FC-BGC}}$ (Pg C K ⁻¹)	-10.06	-25.47	-39.37
γ_L^{RAD} (Pg C K ⁻¹)	-21.09	-36.54	-48.25
$\gamma_L^{\text{FC-BGC}}$ (Pg C K ⁻¹)	-14.05	-26.69	-44.77
$g(\beta_{O}^{\text{BGC}}, \gamma_O^{\text{RAD}})$	0.056	0.075	0.101
$g(\beta_{O}^{\text{FC-RAD}}, \gamma_O^{\text{RAD}})$	0.056	0.075	0.104
$g(\beta_{O}^{\text{BGC}}, \gamma_L^{\text{FC-BGC}})$	0.054	0.087	0.139
$g(\beta_{O}^{\text{FC-RAD}}, \gamma_L^{\text{FC-BGC}})$	0.053	0.087	0.144
$g(E_C^{\text{BGC}}, E_C^{\text{FC}})$	0.051	0.084	0.143

Driving Mechanisms of Nonlinear Land Responses

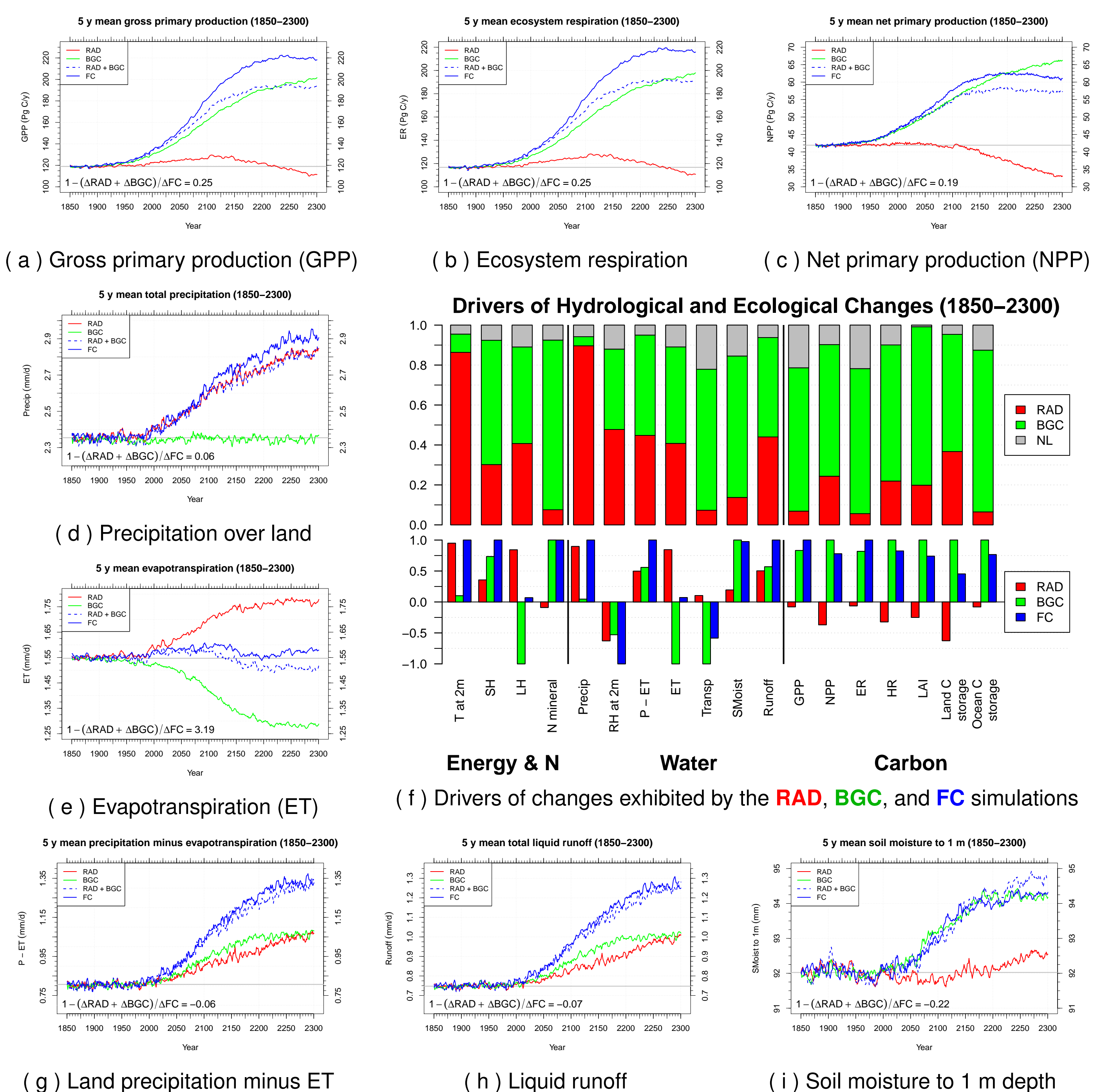


Figure 4: (a) The gross primary production (GPP) of the FC simulation exhibited larger than expected gains under the combined conditions of increasing temperature and elevated CO₂. (b) The trajectories of ecosystem respiration (ER) for all three simulations correspond well with and were slightly lower than GPP. (c) The net primary production (NPP) for the FC simulation cross that of the BGC simulation just before 2200 due primarily to hydrological imbalances in regions where strong drying was expected to occur. (d) Precipitation over land increased as a result of strong temperature increases in the RAD and FC simulations, with no appreciable change seen in the BGC simulation. After 2100, the FC simulation exhibited higher than expected precipitation, likely driven by increases in recycling attributable to gains in canopy evaporation. (e) Correspondingly, the FC simulation exhibited larger than expected evapotranspiration (ET). (f) Shown are the most significant drivers of hydrological and ecological changes exhibited by the RAD, BGC, and FC simulations. (g) Despite the lack of increasing precipitation in the BGC simulation, net P - ET was slightly above that of the RAD simulation. (h) Trajectories of total liquid runoff corresponded well with trajectories of P - ET. (i) The FC and BGC simulations exhibited similar trajectories of soil moisture to 1 m depth.

Discussion and Conclusions

- We found that climate-carbon sensitivities (γ) derived from radiatively (RAD) coupled simulations produced a net ocean carbon storage climate sensitivity that was **weaker** and a net land carbon storage climate sensitivity that was **stronger** than those diagnosed from the fully coupled (FC) and biogeochemically coupled (BGC) simulations.
 - For the ocean, this nonlinearity was associated with warming-induced **weakening of ocean circulation and mixing** in the radiatively coupled (RAD) simulation that limited exchange of dissolved inorganic carbon between surface and deeper water masses.
 - For the land, this nonlinearity was associated with **strong gains in gross primary production** in the fully coupled (FC) simulation, driven by enhancements in the hydrological cycle and increased nutrient availability.
- We developed and applied a **nonlinearity metric** to diagnose the degree to which radiatively (RAD) and biogeochemically (BGC) coupled results produce the fully coupled (FC) result in model responses and driver variables.
- The climate-carbon cycle feedback gain (g) at 2300 was **42% higher** when estimated from climate-carbon sensitivities derived from the difference between the fully coupled and biogeochemically-only coupled simulations than when derived from the radiatively-only coupled simulation.
- Our results suggest that **comparable estimates of the climate-carbon cycle feedback gain (g)** should be calculated from temperature sensitivity parameters (γ) derived from the **combination of fully (FC) and biogeochemically (BGC) coupled simulations**.
- Underestimating the climate-carbon cycle feedback gain (g)** would result in allowable emissions estimates **too low to meet climate change targets**.

Acknowledgements

This research was supported by the Biogeochemistry-Climate Feedbacks Scientific Focus Area (SFA), which is sponsored by the Regional and Global Climate Modeling (RGCM) Program in the Climate and Environmental Sciences Division (CESD) of the Biological and Environmental Research (BER) Program in the U. S. Department of Energy Office of Science. This research used resources of the Oak Ridge Leadership Computing Facility (OLCF) at Oak Ridge National Laboratory (ORNL), which is managed by UT-Battelle, LLC, for the U. S. Department of Energy under Contract No. DE-AC05-00OR22725. The Lawrence Berkeley National Laboratory is managed by the University of California for the U. S. Department of Energy under Contract No. DE-AC02-05CH11231. The National Center for Atmospheric Research (NCAR) is sponsored primarily by the National Science Foundation.